IEEE Access
Multidisciplinary ⋮ Rapid Review ⋮ Open Access Journal

Received 22 March 2023, accepted 8 April 2023, date of publication 11 April 2023, date of current version 17 April 2023.

Digital Object Identifier 10.1109/ACCESS.2023.3266375

RESEARCH ARTICLE

Resource Configuration for Throughput Maximization in UAV-WPCN With Intelligent Reflecting Surface

LIANG XUE[1], (Member, IEEE), XUAN GONG[1], (Student Member, IEEE), YANYAN SHEN[2], (Member, IEEE), BALAJI PANCHAL[3,4], CHUN-JIE WANG[1,2], AND YAN-LONG WANG[5]

[1]School of Information and Electrical Engineering, Hebei University of Engineering, Handan 056038, China
[2]Institute of Advanced Computing and Digital Engineering, Shenzhen Institute of Advanced Technology Chinese Academy of Science, Shenzhen 518055, China
[3]Department of Biochemistry, Dr. Babasaheb Ambedkar Marathawada University, Aurangabad, Maharashtra 431004, India
[4]Key Laboratory of Resource Exploration Research, Hebei University of Engineering, Handan, Hebei 056038, China
[5]Key Laboratory of Trustworthy Distributed Computing and Service, Beijing University of Posts and Telecommunications, Beijing 100876, China

Corresponding author: Yanyan Shen (yy.shen@siat.ac.cn)

This work was supported in part by the Natural Science Foundation of Hebei Province under Grant F2021402009, in part by the Natural Science Foundation of Guangdong Province under Grant 2021A1515011856, in part by the National Natural Science Foundation of China under Grant U1801261 and Grant 61503368, and in part by the Shenzhen Science and Technology Program under grant JCYJ20220818101607015.

ABSTRACT UAV-based wireless powered communication network is a promising method of power supply for battery-free IoT devices, but the limited wireless transmission capability of the UAV constrains the coverage area and transmission throughput. This paper aims to address this issue by exploring intelligent reflecting surfaces with optimized configurations, including the number of reflective elements, transmission power, and the UAV's altitude. The scheme design is challenging because such a throughput maximization problem is essentially a non-convex optimization problem due to the random wireless channel state and the unknown probability distribution of the objective function. By sequentially applying alternating optimization, successive convex approximation, penalty function, and difference-convex optimization, the schemes proposed in this paper can transform the original non-convex optimization problem into a convex one. Extensive evaluation proves the efficacy of the proposed scheme. The paper further compares two settings of the intelligent reflecting surface, namely dynamic phase shift and static phase shift, and provides their performance gap.

INDEX TERMS Wireless powered communication network, intelligent reflecting surface, UAV, alternating optimization.

I. INTRODUCTION

With the development of Internet-of-things (IoT) technology, the number of intelligent wireless devices is increased explosively [1], [2], [3]. However, the large number of batteries used to power these devices presents a serious challenge to both the natural environment and device management. Energy harvesting and wireless power transfer (WPT) [4], [5] together make a promising solution for sustainable IoT [6]systems in the future.

Recently, wireless powered communication network (WPCN) was proposed for the new generation of green loT communication systems [7], [8], [9]. Particularly, the uplink is used for wireless data transfer in a time-division multiplexing manner, while the downlink is purely for power transmission. However, WPCN [10] suffers from several critical limitations. First, the conversion efficiency of WPT degrades significantly as the transmission range increases. Second, the energy conversion efficiency affects the efficiency of wireless

The associate editor coordinating the review of this manuscript and approving it for publication was Yafei Hou.

information transmission (WIT). Increasing the number of antennas for WPT [11] is a straightforward and effective solution but not practical because it incur non-negligible cost increase [12].

Intelligent Reflecting Surfaces (IRS), also known as reconfigurable intelligent surfaces (RIS), are developed using metamaterial technology [13] and are usually packaged with programmable electromagnetic surface structures. IRS consists of a large amount of low-cost subwavelength metal reflecting elements forming a two-dimensional planar array. Each element can independently and intelligently adjust parameters such as the reflected amplitude, phase, polarization, and frequency of an incident signal [14], allowing the target user to gather precise information about wireless signal propagation characteristics and enjoy a better quality of service. Additionally, because each reflective element is small, the IRS has malleable shape and scales well to almost all mounting surfaces. According to the survey in [15], a slab of IRS with 100*102 reflective elements can be as small as $1.02m^2$. It can be easily mounted to the surface of scattering bodies in the complex wireless propagation environment, such as the outer walls of buildings, indoor ceilings, and vehicle surfaces. IRS can improve the efficiency of both power and data transfer in WPCN since its high passive beamforming gain can achieve optimal downlink energy beams and strengthen uplink received signals with low complexity and cost. To further enhance the transmission rate of information, this paper explores unmanned aerial vehicles(UAVs) as a hybrid access point (HAP).

In the past decade, UAV has been widely used as an aerial access point in emergency rescues and aerial surveillance [16], [17], [18], [19]. The UAV-based AP significantly outperforms the traditional fixed AP in terms of mobility, flexibility, and deployment, especially in hazardous monitoring spots, and can guarantee continuous line-of-sight (LoS) link. UAVs with advanced transceivers have attracted a lot of attention for its potential applications in data relaying, information transferring, and sharing [20]. UAVs can also act as wireless energy transmitters to charge low-power wireless devices deployed on the ground [21]. Taking advantage of its highly controllable flexibility, the UAVs can adjust their incident angle over time to shorten the distance to target users on the ground and provide better wireless connections, which provide an appropriate back-up to the WIT and WPT. UAVs in WPCN have been proven to be a promising solution to the energy-constraint of wireless devices. Chen et al. in [22] discusses UAV-enabled WPCNs, in which UAVs are used to harmonize information transfer and energy transmission between a pair of nodes and to minimize the total time consumption to collect the required amount of data at both nodes.

A. RELATED LITERATURE AND MOTIVATION

Considering both IRS and UAV's characteristics and advantages, these two technologies can be merged mutually for the WPCN system to cooperatively enhance the coverage and efficiency of both WPT and WIT. The contributive research efforts related to such pioneering works have been reported in [8], [23], [24], [25], [26], and [27]. To maximize the total network throughput, Hua et al. [8] evaluate influencing factors such as the time allocation, HAP transmission power, and IRS phase shift of full-duplex IRS-WPCN in three different phase shift configurations. The fully dynamic IRS beamforming is firstly proposed that the IRS phase shift vector varies with each time slot during DL WPT and UL WIT. However, the existing works are idealistically thought to be constrained by the linear energy harvesting model, which neglects the channel randomness. Reference [23] studied the self-sustainable hybrid-relaying scheme of IRS-WPCN network, and equipped IRS with an active energy supply unit, so that it can operate for a period of time without HAP energy supply. In [24], under the imperfect channel state information and nonlinear energy harvesting model, the hybrid access point assisted WPCN network is studied, and the provided energy by HAP is minimized. However, although the literatures [8], [23] or [24] have considered the situation where the base station is on the ground, but it would cause the 'double near-far' problem. This problem is in fact an unfair energy harvesting problem caused by the different distances between the base station and the device. UAV's participation can alleviate such a 'double near-far' problem to some extent. In [25], the RF wireless energy transmission method is adopted in the UAV-WPCN network. The UAV transmits the RF energy signal to the wireless device and receives the data information returned by the device. Two schemes of harvest-and-use and harvest-store-use are designed. However, only a single wireless device case was considered in [25] where the UAV trajectory is fixed to a line segment without optimizing the flight track. A multi-agent deep Q learning (DQL) strategy [26] is used to optimize the UAV's flight speed, trajectory, transmission power, and channel resource allocation to maximize the system's minimal throughput. Such deep learning strategy improves the lower bound of the unmanned aerial vehicle-wireless powered communication network (UAV-WPCN) performance. However, IRS as an innovative material technique is not introduced to the scenario in [26], so the potentially further improvement of WPCN network performance remains unexplored. The IRS-assisted UAV-SWIPT system is studied in [27], and the overall downlink information transmission rate of the UAV-SWIPT system is improved by using the alternating optimization (AO) algorithm, through which the variables are optimized in four time blocks. The AO optimization framework is validated effective for SWIPT networks, and the attempt application paves the way for its extension and trial in the WPCN networks.

The combining of UAV and IRS has broaden the network coverage, improved energy efficiency, and increased link capacity of WPCN network. Nevertheless, IRS-assisted UAV-WPCN has not been fully studied, and rare results on the study of network throughput expansion has been reported. Distinguished from the idealized linear energy harvesting

model, which is often too idealistic to model the practical energy consumption behavior. The nonlinear model gradually attracts more research concerns. In the paper, the network throughput maximization is considered in IRS-assisted UAV-WPCN with nonlinear energy harvesting model. In the following, the distinct contributions are given to conclude the advantages of our proposal.

B. CONTRIBUTIONS

The main contributions of this paper are summarized as follows:

- By optimizing the UAV's flight track and other critical parameters, the network throughput is maximized in wireless powered communication networks with the aid of IRS. The throughput maximization problem is proved to be essentially a non-convex optimization problem.
- Several creative mathematical tactics comprehensively cooperate with each other to obtain a tractable problem. The resource configuration at the optimization solution reveals how the maximal throughput can be reached.
- The proposal with dynamic phase shift scheme obtains a higher network throughput than that with the static phase shift scheme.

C. NOTATIONS AND ORGANIZATION

In the paper, the lowercase letter x represents scalar, bold lowercase letter $\mathbf{x}$ represents a vector, and the bold uppercase letter $\mathbf{X}$ represents a matrix. |x| denotes the absolute value of the complex scalar x, $\|\mathbf{x}\|$ marks the Euclidean norm of the complex vector x. $Diag(\mathbf{x})$ represents a diagonal array, where the diagonal elements are the corresponding elements in the vector $\mathbf{x}$. Given a square matrix $\mathbf{X}$, $tr\ (\mathbf{X})$, $rank\ (\mathbf{X})$, $\mathbf{X}^H$, and $[\mathbf{X}]_{m,n}$ denote the trace, rank, conjugate transpose, and the m-th row, n-th column element of the matrix $\mathbf{X}$, respectively. $\mathbf{X} \succcurlyeq 0$ means that $\mathbf{X}$ is a semi-positive definite matrix. $\mathbb{C}^{M\times N}$ denotes a $M \times N$-dimensional complex matrix $\mathbb{C}$. j indicates the imaginary unit, i.e. $j^2 = -1$. $E\{\}$ represents the mathematical expectation operation. The distribution of a circularly symmetric complex Gaussian (CSCG) matrix $\mathbf{X}$ with its mean μ and covariance matrix C is denoted as $\mathbf{X} \sim CN(\mu, C)$, '$\sim$' refers to 'distribution for'.

The paper is organized as follows, Section II describes the network model and formulates the network throughput maximization problem considering dynamic phase shift scheme of IRS. Section III describes the problem transformation and the procedures to obtain the solution within the framework of alternating optimization. In section IV, the solution to the optimization problem considering the static phase shift of IRS is proposed. In section V, the numerical results show the effectiveness of the proposed algorithm. The conclusions and future research direction are presented in Section VI.

II. SYSTEM MODEL AND PROBLEM FORMULATION

A. NETWORK MODEL

Fig.1 illustrates a typical IRS-assisted UAV-WPCN network. The network consists of a single-antenna UAV acting as a HAP, an IRS with M reflective elements, and K wireless intelligent devices. In this paper, 'HAP' and 'UAV' have identical meanings and will be designated interchangeably. Meanwhile, network throughput and the sum of achieved data transmission rate are also of the same definition. All K wireless intelligent devices planted on the ground are assumed operating in their fully passive mode. Noticeably, they have no built-in battery to sustain themselves and must harvest energy from the HAP's RF broadcasting signals. The IRS is mounted on the outer wall of the nearby towering architecture to assist the RF energy transmission by reflecting RF signals from the UAV to K wireless devices and the data transmission by transferring the required data from K wireless devices to the UAV. For brevity, the network modeled in the paper follows HTT (harvest and then transmit) protocol [10]. In phase of the downlink wireless power transfer (DL-WPT), K wireless devices first harvest the RF energy from the HAP, and then deplete the scavenged power in phase of the uplink wireless information transmission (UL-WIT). These wireless devices make use of the converted energy from the HAP's RF signals to transfer locally collected data to the HAP. Due to channel reciprocity, signals in phases of DL-WPT and UL-WIT experience the same level of channel fading. The quasi-static flat-fading channel models characterize both the channel gains in UL-WIT and DL-WET links. The channel coefficients are reasonably assumed maintaining constant during each short time slot but could vary from slot to slot. All channel state information (CSI) are assumed to be known in advance at the HAP, so the achievable performance to be explored herein is practically a theoretical upper bound of the actual performance. Due to the IRS's low manufacturing cost and tiny energy expense, its computation capability is usually constrained. Therefore, the IRS needs the HAP to assist it in calculating the optimal phase shift, which helps each reflective element work in the optimized state, and thus is beneficial to improving the transmission performance.

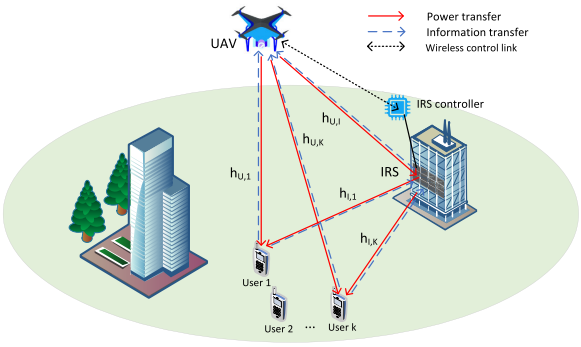

FIGURE 1. The information and energy flows in the WPCN.

The k-th device's coordinate can be described by its Cartesian 3D coordinate $w_k = [x_k, y_k, 0]^T, k = 1, \ldots, K$, where x_k and y_k are the horizontal and vertical axises, respectively. As to the IRS, the coordinate of the i-th reflective element is denoted as $w_i = [x_i, y_i, h_i]^T, i = 1, \ldots, M$, where x_i, y_i

are the coordinate of the horizontal and vertical axises, and h_i denotes its centroid height. The UAV's total flight time T can be equally divided into N time slots, and for any time slot n, $n \in \{1, 2, \ldots, N\}$, its time duration is defined as $\delta = T/N$. The duration of each slot will be infinitely short as $N \to +\infty$. The UAV keeps flying parallelly to the ground at its maximum horizontal speed v_{max}. Since the duration of each time slot can be set to be very short, the UAV's relative position to the ground can be regarded stationary during each time slot. Therefore, the coordinate of the UAV in time slot n can be denoted as $L[n] = [x[n], y[n], z]^T, n = 1, \ldots, N$, where z indicates the fixed flight height. The flight height is predefined as the lowest altitude at which the UAV can avoid colliding with the nearby buildings and ensure the stability of its downlink connections with K devices on the ground. The starting and ending points of the UAV can be represented by L_I and L_F, respectively. The flight track of the UAV simultaneously satisfies the following constraints

$$L_I = L[1], \tag{1}$$

$$L_F = L[N], \tag{2}$$

$$||L[n+1] - L[n]||^2 \leq (v_{\max}\delta)^2, n = 1, \ldots, N-1. \tag{3}$$

B. CHANNEL MODEL

The channel gains of the links originating from the UAV to the IRS, from the IRS to the device k, and from the UAV to device k are denoted by $h_{U,I} \in \mathbb{C}^{M\times 1}, h_{I,k}^H \in \mathbb{C}^{1\times M}$ and $h_{U,k}^H \in \mathbb{C}$, respectively. To explore the upper bound of the network performance for WPCN, the CSI of all channels defined in the paper is assumed to be acquired beforehand for simplifying the formulation of a joint dynamic beamforming and resource allocation optimization problem [28]. Since the UAV flies or hovers stably at a fixed height and the IRS is placed on the outer wall of the building, no other visible objects can block the links between the UAV and the IRS, LoS link can be established between them. On the other hand, both the channels from the IRS to device k, and from the UAV to device k, can be modeled as Rice channels, because the received signal at the device k contains both LoS and multipath signals that arrive from scattering directions due to object reflections [29].

The LoS component relevant to the IRS can be represented by the response of a uniform linear array (ULA) of antennas. In the n-th time slot downlink transmission, the ULA response vector can be expressed by

$$\boldsymbol{a}[n] = [1, e^{-j2\pi\frac{d}{\lambda}\cos\phi[n]}, \ldots, e^{-j2\pi(M-1)\frac{d}{\lambda}\cos\phi[n]}]^T, \forall n, \tag{4}$$

where $\phi[n]$ denotes the angle of arrival (AoA) from the UAV to the IRS in the n-th time slot, and $\cos\phi[n] = \frac{x_i - x[n]}{||L[n]-w_i||}$, λ indicates the wavelength, d represents the distance between two adjacent reflective elements. Therefore, the channel gain of the LoS link from the UAV to the IRS in the n-th time slot can be expressed as

$$h_{U,I}[n] = \sqrt{\frac{\beta_0}{||L[n] - w_i||^2}}\boldsymbol{a}[n], \forall n, \tag{5}$$

where β_0 represents the reference path loss at a distance of 1 meter. Meanwhile, the channel gain between the UAV and device k in the n-th time slot can be expressed as [24]

$$h_{U,k}[n] = \sqrt{\frac{\beta_0}{||L[n] - w_k||^\alpha}}\left(\sqrt{\frac{\kappa_1}{1+\kappa_1}}h_{U,k}^{LoS}[n] + \sqrt{\frac{1}{1+\kappa_1}}h_{U,k}^{NLoS}[n]\right), \forall k, n, \tag{6}$$

where α is the path loss index of the channel from UAV to device k (named as U-K channel for short), and κ_1 is the Rice factor, $h_{U,k}^{LoS}[n] = 1$, and $h_{U,k}^{NLoS}[n] \sim CN(0, 1)$ denotes the random scattering component. Similarly, the channel gain $h_{I,k}$ of the link between the IRS and the wireless device k can be expressed as

$$h_{I,k} = \sqrt{\frac{\beta_0}{||w_i\text{-}w_k||^\gamma}}\left(\sqrt{\frac{\kappa_2}{1+\kappa_2}}h_{I,k}^{LoS} + \sqrt{\frac{1}{1+\kappa_2}}h_{I,k}^{NLoS}\right), \forall k, \tag{7}$$

where γ is the path loss index associated with the channels from the IRS to device k (named I-K channels for short), and κ_2 is the Rice factor. Since the direct channel is related to the IRS, the corresponding LoS component can be expressed as

$$h_{I,k}^{LoS} = [1, e^{j2\pi\frac{d}{\lambda}\cos\varphi_k}, \ldots, e^{j2\pi\frac{d}{\lambda}(M-1)\cos\varphi_k}]^T, \forall k, \tag{8}$$

where φ_k is the angle of departure of the information on the channel from the IRS signal to the k-th wireless device, $\cos\varphi_k = \frac{x_k - x_i}{||w_i - w_k||}$, $h_{I,k}^{NLoS} \sim CN(0, I_M)$, I_M denotes the unit vector.

For an IRS with M reflecting elements, each reflecting element can independently adjust the reflection amplitude and the phase of the incident signal, so the reflection coefficient matrix at the IRS can be expressed in the form of a diagonal array, i.e., $\Theta[n] = diag(\beta_1[n]e^{j\theta_1[n]}, \ldots, \beta_m[n]e^{j\theta_m[n]}, \ldots, \beta_M[n]e^{j\theta_M[n]})$, where $\beta_m[n] \in [0, 1]$ and $\theta_m[n] \in [0, 2\pi)$ represent the amplitude and phase shift of the m-th reflection element, respectively. Since $\beta_m[n] = 1$, $m \in \{1, \ldots, M\}$ can achieve the maximum amplitude, let $\beta_m[n] = 1$ be uniformed throughout the paper. Then the reflection coefficient matrix in DL-WET and UL-WIT can be expressed by $\Theta_0[n] = diag(e^{j\theta_{0,1}[n]}, \ldots, e^{j\theta_{0,M}[n]})$, and $\Theta_k[n] = diag(e^{j\theta_{k,1}[n]}, \ldots, e^{j\theta_{k,M}[n]}), k \in 1, \ldots, K$, respectively. Let $e^{j\theta_{0,m}[n]} = e_{0,m}[n], \forall m$, $e^{j\theta_{k,m}} = e_{k,m}[n], \forall k, m$. The phase shift constraint for the reflecting elements of the IRS in the DL-WET and UL-WIT can be expressed as follows respectively,

$$|e_{0,m}[n]| = 1, \forall m, n, \tag{9}$$

$$|e_{k,m}[n]| = 1, \forall k, m, n. \tag{10}$$

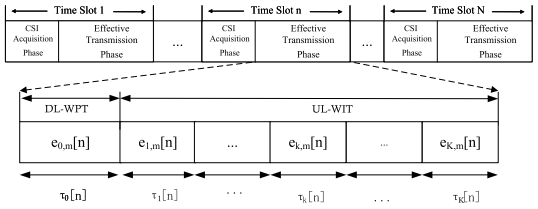

FIGURE 2. Dynamic IRS phase shift within time slot *n*.

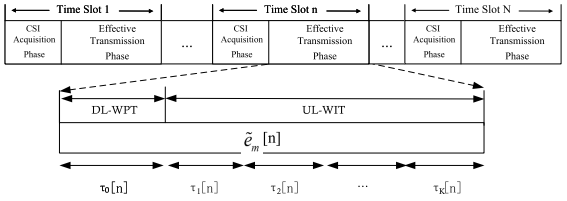

FIGURE 3. Static IRS phase shift within time slot *n*.

C. TRANSMISSION MODEL

The HTT protocol is applied for energy harvesting and data transmission. In general, the time required for CSI acquisition is significantly smaller than that of the effective transmission phase [30]. Consequently, in this paper, the time required for CSI acquisition is disregarded in the time constraints. In each time slot, the UAV first transmits RF energy in form of broadcasting signals to the devices on the ground via the DL-WET link in the allocated time segment $\tau_0[n]$. All wireless devices harvest RF energy during the time segment of $\tau_0[n]$, and then the k-th wireless device transfers the collected sensing data to the UAV via UL-WIT links in the allocated time segment $\tau_k[n]$. Since the duration of each time slot is limited, the time segments constraint should satisfy $\tau_0[n]+\tau_1[n]+\ldots+\tau_K[n] \leq \delta$.

The IRS elements' phase shift can keep uniform or vary in the downlink or the uplink transmissions within a time slot. Therefore two different IRS phase shift scenarios, the dynamic IRS phase shift and the static IRS phase shift are studied in the paper. In the dynamic IRS phase shift settings, i.e., the phase shift of IRS can be adjusted with respect to each time slot e.g., $\tau_k[n]$, $k \in \{0, 1, \ldots, K\}$, while in the static IRS phase shift scenario, the phase shift of the IRS keeps uniform within time slot n. To clearly describe the two scenarios, the dynamic IRS phase shift and the static IRS phase shift are illustrated in Fig.2 and Fig.3, respectively. Fig.2 shows a dynamic phase shift in the n-th time slot, in which the phase shift settings for energy and information can be dynamically tuned to meet each segment's needs. Fig.3 shows a static phase shift configuration in the n-th time slot, in which the phase shift configurations keep unvaried irrespective of the available segments. In view of channel estimation and cost-cutting, the IRS is thought to be equipped with an extreme low-power receive RF chain [31], which enables IRS to sense the real time channel state. Therefore, the CSI information can be obtained by the HAP, and then it is transmitted from the HAP to the IRS controller through the wireless control link, thereby changing the phase shift of the IRS. For these two phase shift schemes, CSI is successively updated at the very beginning of each time slot to respond to the real-time phase shift change. The CSI acquisition phase is also indispensable to the implementation of dynamic phase shift scheme.

In the DL-WPT link, the HAP broadcasts RF signal using constant transmission power P_0 to K wireless devices during the time segment $\tau_0[n]$. Considering that the noise power is much less than the HAP RF signal power, the RF energy harvested from the RF noises can be negligible. The received power $P_k^{DL}[n]$ at the k-th wireless device in the n-th time slot is given by,

$$P_k^{DL}[n] = P_0|h_{U,k}[n] + h_{I,k}\Theta_0[n]h_{U,I}[n]|^2. \tag{11}$$

To accurately count the RF energy harvested by the k-th wireless device, a non-linear energy harvesting model better fit to reality is employed to be more coincidental with practice [32]. The energy collected by the k-th wireless device can be expressed as

$$\Xi(P_k^{DL}[n]) = \frac{A}{X_k(1+\exp(-a_k(P_k^{DL}[n]-b_k)))} - Y_k, \forall k, \tag{12}$$

where $X_k = \exp(\frac{a_k b_k}{1+\exp(a_k b_k)})$ and $Y_k = \frac{A}{\exp(a_k b_k)}$. The constant A indicates the maximum received power of the EH receiver when the EH circuit is saturated, a_k and b_k are parameters related to the circuit designing components, such as resistance, capacitance, and the breakover voltage of the diode. Curve fitting tools can help find typical values of these three parameters, i.e., A, a_k, b_k. Accordingly, the amount of energy collected by wireless device k during time segment $\tau_0[n]$ can be expressed as

$$E_k[n] = \tau_0[n]\Xi(P_k^{DL}[n]). \tag{13}$$

The wireless devices transmit locally data to UAV by using the collected energy during the UL-WIT transmission. The transmitted signal of the k-th device is

$$d_k = \sqrt{P_k^{UL}[n]}s_k^{UL}[n], \forall k, n, \tag{14}$$

where $P_k^{UL}[n]$ is the transmission power of the k-th device in the n-th time slot and $s_k^{UL}[n] \sim CN(0,1)$ is the transmitted information signal. The energy consumed by each device for the uplink information transmission should be no more than the collected energy during the DL-WET, so the following available energy constraint should be satisfied

$$\tau_k[n]P_k^{UL}[n] \leq E_k[n]. \tag{15}$$

In the phase of UL-WIT, the received signals by the HAP through both the direct and indirect links can be synthesized as

$$y = \sum_{k=1}^{K}(h_{U,k}[n] + h_{I,k}\Theta_k[n]h_{U,I}[n])d_k + \bar{n}, \tag{16}$$

where $\bar{n} \in \mathbb{C}^{1\times M}$ denotes the additive white Gaussian noise (AWGN) introduced by the HAP receiving antenna, assuming that $\bar{n} \sim CN(0, \sigma^2)$. The signal-to-noise ratio (SNR) of the k-th wireless device in the n-th time slot can be expressed as

$$SNR_k[n] = \frac{P_k^{UL}[n]|h_{U,k}[n] + h_{I,k}\Theta_k[n]h_{U,I}[n]|^2}{\sigma^2}. \quad (17)$$

As a result, the achievable information rate by the k-th device at time slot n can be expressed as $R_k[n] = \log_2(1 + SNR_k[n]), \forall k, n$. The network throughput achieved by all K devices in the time period T can be given by

$$R_{sum} = \sum_{n=1}^{N}\sum_{k=1}^{K} \tau_k[n]R_k[n] = \sum_{n=1}^{N}\sum_{k=1}^{K} \tau_k[n]\log_2\left(1 + \frac{P_k^{UL}[n]|h_{U,k}^H[n] + h_{I,k}\Theta_k[n]h_{U,I}[n]|^2}{\sigma^2}\right). \quad (18)$$

D. PROBLEM FORMULATION

In the paper, the sum rate of K devices is maximized by simultaneously optimizing flight track $L = \{L[n], \forall n\}$ of the UAV, the IRS phase shift of the downlink $e_0 = \{e_{0,m}[n], \forall m, n\}$, the IRS phase shift of the uplink $e_k = \{e_{k,m}[n], \forall k, m, n\}$, the time segment for energy transmission $\tau_0 = \{\tau_0[n], \forall n\}$, the time segment $\tau_k = \{\tau_k[n], \forall k, n\}$ for information transmission, and the transmission power of the wireless device $P_k^{UL} = \{P_k^{UL}[n], \forall k, n\}$. The optimization problem P0 can be formulated as follows,

$$\text{P0}: \max_{e_0, e_k, \tau_0, \tau_k, P_k^{UL}, L} R_{sum}, \quad (19a)$$

$$s.t. \quad L_I = L[1], \quad (19b)$$

$$L_F = L[n], \forall n, \quad (19c)$$

$$||L[n+1] - L[n]||^2 \le (v_{\max}\delta)^2, \quad n = 1, \ldots, N-1, \quad (19d)$$

$$\tau_k[n]P_k^{UL}[n] \le E_k[n], \quad (19e)$$

$$\tau_0[n] + \sum_{k=1}^{K} \tau_k[n] \le \delta, \quad (19f)$$

$$|e_{0,m}[n]| = 1, \forall m, \quad (19g)$$

$$|e_{k,m}[n]| = 1, \forall k, m, \quad (19h)$$

$$\tau_0[n] \ge 0, \tau_k[n] \ge 0, P_k^{UL}[n] \ge 0, \forall k. \quad (19i)$$

The constraints (19b)-(19d) represent the UAV's trajectory constraint. The inequality constraint (19e) indicates that the energy consumption on the uplink data transmission of device k should be less than its harvested energy purely from the RF signal. The constraint (19f) represents that the total duration of time segments should be no more than the predefined time slot δ. The constraint (19g) represents the phase shift constraint on the downlink data transmission. The constraint (19h) represents the phase shift constraint on the uplink data transmission, and the constraint (19i) indicates that the optimization variables cannot be negative. Due to the complex coupling relationships between the optimization variables, the objective function is not jointly concave, and the constraint set is non-convex. Thus the optimization problem P0 is non-convex. Finding an efficient solution using conventional methods is difficult, so the alternating optimization (AO) algorithm is introduced to solve this optimization problem [33], [34].

III. PROBLEM TRANSFORMATION AND AO ALGORITHM DESIGN

In problem P0, random variables appear in the objective function, which makes the problem difficult to solve directly. To make the problem easy to solve, the objective function is transformed by using mathematical expectation. However, the transformed problem is still non-convex, so the AO based algorithm is proposed. The AO based algorithm divides the transformed problem into four subproblems, each of which is solved separately.

A. PROBLEM TRANSFORMATION

Since the probability distribution of R_{sum} is hard to acquire beforehand, it is not easy to find a closed-form solution for P0. However, since the objective function of the optimization problem P0 contains random variables, the mathematical expectation $E\{R_{sum}\}$ can be applied in the problem transformation. The following lemma 1 can be used to approximate the probability distribution of R_{sum}.

Lemma 1: If X is a positive random variable, for $\forall \psi > 0, \varphi > 0$, the following approximate expression holds,

$$E\{\log_2(1 + \frac{\psi X}{\varphi})\} \approx \log_2(1 + \frac{\psi E\{X\}}{\varphi}). \quad (20)$$

Proof: Please see the appendix for proof. The proof of Lemma 1 is completed.

Let $H_k[n] = |h_{U,k}[n] + h_{I,k}\Theta_k[n]h_{U,I}[n]|^2$, the following transformations can be used to obtain the mathematical expectation of $H_k[n]$,

$$\begin{aligned} &E\{H_k[n]\} \\ &= E\{|h_{U,k}^I[n] + h_{U,k}^{II}[n] + (h_{I,k}^I + h_{I,k}^{II})\Theta_k[n]h_{U,I}^H[n]|^2\} \\ &= E\{|h_{U,k}^I[n] + h_{I,k}^I\Theta_k[n]h_{U,I}^H[n]|^2\} + E\{|h_{U,k}^{II}[n]|^2\} \\ &+ E|h_{I,k}^{II}\Theta_k[n]h_{U,I}^H[n]|^2 \\ &= \frac{\beta_0 - v_1}{||L[n] - w_k||^\alpha} + \frac{M\beta_0(\beta_0 - v_2)}{||L[n] - w_i||^2||w_i - w_k||^\gamma} \\ &+ |h_{U,k}^I[n] + h_{I,k}^I\Theta_k[n]h_{U,I}^H[n]|^2 \triangleq \xi, \end{aligned} \quad (21)$$

where

$$h_{U,k}^{I}[n]=\sqrt{\frac{v_1}{||L[n]-w_k||^{\alpha}}}h_{U,k}^{LoS}[n],\ v_1=\frac{\beta_0\chi_1}{1+\chi_1},$$
$$h_{U,k}^{II}[n]=\sqrt{\frac{\beta_0-v_1}{||L[n]-w_k||^{\alpha}}}h_{U,k}^{NLoS}[n],\ v_2=\frac{\beta_0\chi_2}{1+\chi_2},$$
$$h_{I,k}^{I}=\sqrt{\frac{v_2}{||w_i-w_k||^{\gamma}}}h_{I,k}^{LoS},\ h_{I,k}^{II}=\sqrt{\frac{\beta_0-v_2}{||w_i-w_k||^{\gamma}}}h_{I,k}^{NLoS}.$$

According to Lemma 1, it can be shown that

$$E\{R_k[n]\}=E\{\log_2(1+\frac{P_k^{UL}[n]E\{H_k[n]\}}{\sigma^2})$$
$$=\log_2(1+\frac{P_k^{UL}[n]\xi}{\sigma^2})\triangleq\tilde{R}_k[n]. \quad (22)$$

Substitute Eq.(22) to the optimization problem P0, the updated objective function yields and is shown as

$$\tilde{R}_{sum}=\sum_{n=1}^{N}\sum_{k=1}^{K}\tau_k[n]\tilde{R}_k[n]. \quad (23)$$

B. OPTIMIZATION OF UAV FLIGHT TRAJECTORY

Given the downlink IRS phase shift e_0, uplink IRS phase shift e_k, time segment τ_0 for energy transfer, time segment τ_k for information transmission, and information transmission power of the wireless device P_k^{UL}, the optimization problem for solving the UAV's flight trajectory can be formulated as problem P1:

$$\text{P1}:\max_{L}\tilde{R}_{sum}, \quad (24a)$$
$$s.t.\ (19b)\text{-}(19e). \quad (24b)$$

The optimization problem P1 remains a non-convex optimization problem since the constraint (19e) is non-convex. The auxiliary variables need to be introduced to help further transform it. Denote $\{U_k>0,\forall k\}$ as the upper limit of $||L[n]-w_k||$ and $\{U_r>0\}$ as the upper limit of $||L[n]-w_i||$, i.e.,

$$U_k^2\geq||L[n]-w_k||^2, \quad (25)$$
$$U_r^2\geq||L[n]-w_i||^2. \quad (26)$$

So the lower bound of ξ can be obtained as

$$\xi^{lb}=\frac{\beta_0}{U_k^{\alpha}}+\frac{\alpha_k}{U_r^2}+\frac{\beta_k}{U_k^{\alpha/2}U_r}, \quad (27)$$

where $\alpha_k=\beta_0|h_{I,k}^{I}\Theta_k[n]\boldsymbol{a}[n]|^2+\frac{M\beta_0(\beta_0-v_2)}{||w_i-w_k||^{\gamma}}$ and $\beta_k=2\,\text{Re}\{\sqrt{v_1\beta_0}h_{I,k}^{I}\Theta_k[n]\boldsymbol{a}[n]\}$. Define the auxiliary variable C_k

$$C_k=\sigma^2/\xi^{lb}. \quad (28)$$

Therefore, the lower bound of the objective function of the optimization problem P1 can be formulated as

$$\tau_k[n]\tilde{R}_k[n]\geq\tau_k[n]\log_2(1+\frac{P_k^{UL}[n]}{C_k}). \quad (29)$$

Thus problem P1 can be equivalently transformed to P1.1:

$$\text{P1.1}:\max_{L,\Psi}\sum_{n=1}^{N}\sum_{k=1}^{K}\tau_k[n]\log_2(1+\frac{P_k^{UL}[n]}{C_k}), \quad (30a)$$
$$s.t.\ P_k^{DL}[n]\geq\Xi^{-1}(\frac{\tau_k[n]}{\tau_0[n]}P_k^{UL}[n]), \quad (30b)$$
$$C_k\geq\sigma^2/\xi^{lb}, \quad (30c)$$
$$(19b)\text{-}(19d),(25)\text{-}(27), \quad (30d)$$

where $\Psi=\{U_k,U_r,\xi^{lb},C_k\}$ denotes the set of all the auxiliary variables introduced above. $\Xi^{-1}(x)=b_k-\frac{\ln(A/(x+Y_k)X_k)-1}{a_k}$. (30b) is derived from (13) and (19e). Since the objective function of P1.1 is non-concave and the constraints (25)-(27) are non-convex, the optimization problem P1.1 remains a non-convex optimization problem. Generally, it is challenging to obtain the optimal solution to non-convex problems, thus the successive convex approximation (SCA) method is used to obtain a suboptimal solution to the transformed problem P1.1.

The objective function (30a) can be expressed as $f(C_k)=\sum_{n=1}^{N}\sum_{k=1}^{K}\tau_k[n]\log_2(1+\frac{P_k^{UL}[n]}{C_k})$, which is convex in terms of C_k. Since problem P1.1 aims to find the maximum value of the objective function, the lower bound of the objective function $f(C_k)$ at the point $C_k^{(r)}$ in the r-th iteration.

$$f(C_k)\geq\sum_{n=1}^{N}\sum_{k=1}^{K}\tau_k[n](\log_2(1+\frac{P_k^{UL}[n]}{C_k^{(r)}})-\frac{P_k^{UL}[n](C_k-C_k^{(r)})}{C_k^{(r)}(C_k^{(r)}+P_k^{UL}[n])\ln 2})\triangleq f^{lb}(C_k). \quad (31)$$

For inequalities (25) and (26), their left hand sides can be approximated by their first order Taylor expansion at any given point $U_k^{(r)}$ and $U_r^{(r)}$. After approximation, inequalities (25) and (26) can be written as

$$(U_k^{(r)})^2+2U_k^{(r)}(U_k-U_k^{(r)})\geq||L[n]-w_k||^2,\forall k,\forall n, \quad (32)$$
$$(U_r^{(r)})^2+2U_r^{(r)}(U_r-U_r^{(r)})\geq||L[n]-w_i||^2,\forall k,\forall n. \quad (33)$$

The variable $\phi[n]$ of AoA in the right hand side of Eq.(27) is included in both α_k and β_k, which depend on the position of the drone in the n-th time slot, so the constraint can be introduced as

$$||L[n]-L[n]^{(r)}||\leq\delta_{\max}^2, \quad (34)$$

where $L[n]^{(r)}$ denotes the value of the r-th iteration of SCA and $\delta_{\max}$ indicates the maximum migration distance allowed in the time slot δ. If $\delta_{\max}$ is small enough, it can be assumed that AoA is almost constant after each iteration and therefore α_k, β_k are almost unchanged. The $(r+1)$-th SCA iteration is based on the AoA achieved in the r-th time slot. To ensure the accuracy of the approximation, it is required that the ratio of the maximum migration distance of the n-th time slot to the minimum altitude of the UAV should satisfy: $\delta_{\max}/z_{\min}\leq\iota$,

i.e., $\delta_{\max} \leq \iota z_{\min}$. Due to this constraint, both sides of Eq.(27) depend only on U_k, U_r, so the following lemma 2 is used to solve it.

Lemma 2: $g_1(x_1, x_2) = a_1(x_1)^{-\alpha} + a_2(x_2)^{-2}$, $g_2(x_1, x_2) = a_3(x_1)^{-(\alpha/2)}(x_2)^{-1}$ is jointly convex with respect to x_1, x_2, when $\alpha, a_1, a_2, a_3, x_1, x_2$ are positive.

Proof: When $x_1 > 0, x_2 > 0$, the Hessian matrices of $g_1(x_1, x_2)$, $g_2(x_1, x_2)$ are both semi-positive definite, and therefore both of them are convex functions. The proof of **Lemma 2** is completed.

Then $\xi^{lb} = \tilde{g}(U_k, U_r) + \beta_k\tilde{h}$, where $\tilde{h} = \frac{1}{U_k^{\alpha/2}U_r}$. According to Lemma 2, because of $\beta_0 > 0$ and $\beta_k > 0$, then $\tilde{g}(U_k, U_r) + \beta_k\tilde{h}$ is jointly convex with respect to U_k, U_r. So SCA can be used to obtain the lower bound of $\tilde{g}(U_k, U_r) + \beta_k\tilde{h}$, i.e.,

$$(\tilde{g} + \beta_k\tilde{h})^{lb} = \tilde{g}^{lb} + \beta_k\tilde{h}^{lb}, \tag{35}$$

$$\tilde{g}^{lb} = \beta_0(U_k^{(r)})^{-\alpha} - \alpha(U_k^{(r)})^{-\alpha-1}(U_k - U_k^{(r)}) + \alpha_k(U_r^{(r)})^{-2} - 2\alpha_k(U_r^{(r)})^{-3}(U_r - U_r^{(r)}), \forall k, \tag{36}$$

$$\tilde{h}^{lb} = (U_k^{(r)})^{-\alpha/2}(U_r^{(r)})^{-1} - \alpha/2(U_k^{(r)})^{-\alpha/2-1}(U_r^{(r)})^{-1}(U_k - U_k^{(r)}) - (U_k^{(r)})^{-\alpha-2}(U_r^{(r)})^{-2}(U_r - U_r^{(r)}), \forall k \tag{37}$$

So the constraint (27) can be converted to

$$\xi^{lb} \leq (\tilde{g} + \beta_k\tilde{h})^{lb}, \forall k. \tag{38}$$

After the first-order Taylor expansion and SCA transformation, the optimization problem P1.1 can be reorganized as follows:

$$\text{P1.2}: \max_{L,\Psi} f^{lb}(C_k), \tag{39a}$$

$$s.t.\ (19b)\text{-}(19d),(30b)\text{-}(30c),(32),(33),(38). \tag{39b}$$

In problem P1.2, a standard convex optimization problem can be solved directly by using the CVX toolbox [35].

C. OPTIMIZATION OF UPLINK PHASE SHIFT

Only the uplink IRS phase shift remains to be optimized when the downlink IRS phase shift e_0, information transmission power P_k^{UL}, UAV trajectory L, energy transfer time τ_0, and information transfer time τ_k are all fixed.

Initially, the optimization variable $e_{k,m}[n]$ involves only unit mode constraint (19h) and the objective function (19a). Each $e_{k,m}[n]$ is only associated with one device and is independent of all the other variables, and there are no mutual coupling relationships between $e_{k,m}[n]$ and $e_{j,m}[n]$ $(j \neq k)$. In other words, $e_{k,m}[n]$ can be separated from the optimization problem P0, so that the optimal $e_{k,m}[n]$ for IRS phase shifts can be obtained by solving k subproblems and finally synthesized their optimums into $e_{k,m}[n]$ of the original problem P0. In particular, each optimal $e_{k,m}[n]$ can be found by solving the following problem P2,

$$\text{P2}: \max_{e_k} |(h_{U,k}^I[n])^H + G_k^H[n]e'_{k,m}[n]|^2, \tag{40a}$$

$$s.t.\ |e_{k,m}[n]| = 1, \forall k, m, \tag{40b}$$

where $G_k[n] = (h_{I,k}^I)^H diag(h_{U,I}[n])$ and $e'_{k,m}[n] = [e^{j\theta_{k,1}[n]}, \ldots, e^{j\theta_{k,M}[n]}]^T$. According to [36], this problem should be solved by aligning all IRS reflections and all non-IRS reflection signals to maximize the effective uplink channel power gain, as given by

$$e^*_{k,m}[n] \triangleq e_{k,m}[n] = e^{j(\arg\{(h_{U,K}^I[n])^H\} - \arg\{[G_k[n]]_m\})}, \forall k, m. \tag{41}$$

D. OPTIMIZATION OF TIME ALLOCATION

Given downlink IRS phase shift e_0, uplink IRS phase shift e_k, information transmission power P_k^{UL}, and UAV trajectory L, the optimization problem of solving the energy transfer time τ_0 and information transmission time τ_k can be written as P3, i.e.,

$$\text{P3}: \max_{\tau_0,\tau_k} \tilde{R}_{sum}, \tag{42a}$$

$$s.t.\ \tau_k[n]P_k^{UL}[n] \leq \tau_0[n]\Xi[P_k^{DL}], \tag{42b}$$

$$\tau_0[n] + \sum_{k=1}^{K} \tau_k[n] \leq \delta, \tag{42c}$$

$$\tau_0[n] \geq 0, \tau_k[n] \geq 0, k = 1, \ldots, K. \tag{42d}$$

As can be seen, the objective function $\tilde{R}_{sum}$ is a concave function of $\tau_k[n]$, and the constraints (42b)-(42d) are linear functions about the optimization variables, i.e., $\tau_0[n]$ and $\tau_k[n]$. P3 is still a convex optimization problem and can be solved directly using a toolbox such as CVX.

E. OPTIMIZATION OF DOWNLINK PHASE SHIFT AND UPLINK POWER

When the UAV flight trajectory, IRS uplink phase shift, energy transfer time, and information transmission time are given, the optimization problem for solving the downlink phase shift and uplink power can be expressed as problem P4.

$$\text{P4}: \max_{p_k^{UL}, e_0} \tilde{R}_{sum}, \tag{43a}$$

$$s.t. \quad (19e),(19g), \tag{43b}$$

$$P_k^{UL}[n] \geq 0, \forall k. \tag{43c}$$

Let $H_0[n] = |h_{U,k}[n] + h_{I,k}\Theta_0[n]h_{U,I}[n]|^2$, according to Eq. (21), it can be obtained

$$E\{H_0[n]\} = \frac{\beta_0 - v_1}{||L[n] - w_k||^\alpha} + \frac{M\beta_0(\beta_0 - v_2)}{||L[n] - w_i||^2||w_i - w_k||^\gamma} + |h_{U,k}^I[n] + h_{I,k}^I\Theta_0[n]h_{U,I}^H[n]|^2 \triangleq \xi_0. \tag{44}$$

Let $f_k = diag(h_{U,I}^H[n])h_{I,k}^I$, $\tilde{e}_0 = [e_{0,1}[n], \ldots, e_{0,m}[n]]^H$, thus $|h_{U,k}^I[n] + h_{I,k}^I\Theta_0[n]h_{U,I}^H[n]|^2$ can be written as

$|h^I_{U,k}[n] + \tilde{e}_0^H f_k|^2$. Then we introduce auxiliary variables as

$$V_k = \begin{bmatrix} f_k f_k^H & f_k h^I_{U,k}[n] \\ h^I_{U,k}[n] f_k^H & 0 \end{bmatrix}, \bar{\tilde{e}}_0 = \begin{bmatrix} \tilde{e}_0 \\ 1 \end{bmatrix}. \quad (45)$$

Therefore, $|h^I_{U,k}[n] + \tilde{e}_0^H f_k|^2$ can be further expressed as $\bar{\tilde{e}}_0{}^H V_k \bar{\tilde{e}}_0 + |h^I_{U,k}[n]|^2$. Since $\bar{\tilde{e}}_0{}^H V_k \bar{\tilde{e}}_0 = tr(V_k \bar{\tilde{e}}_0 \bar{\tilde{e}}_0^H)$, then let $E_0 = \bar{\tilde{e}}_0 \bar{\tilde{e}}_0^H$, where $E_0 \succcurlyeq 0$ and the rank one constraint must be satisfied, i.e., $Rank(E_0) = 1$. Thus $\xi_0 = \omega_k + |h^I_{U,k}[n]|^2 + tr(V_k E_0)$, where $\omega_k = \frac{\beta_0 - v_1}{||L[n] - w_k||^\alpha} + \frac{M\beta_0(\beta_0 - v_2)}{||L[n] - w_i||^2 ||w_i - w_k||^\gamma}$. Eq. (11) can be expressed as

$$P_k^{DL}[n] = P_0 \xi_0. \quad (46)$$

In other words, the non-linear energy harvesting behavior depicted in Eq.(12) can be expressed as

$$\Xi(P_0\xi_0) = \frac{A}{X_k(1 + \exp(-a_k(P_0\xi_0) - b_k)))} - Y_k, \forall k. \quad (47)$$

Substituting Eq. (47) to inequality (19e), the following inequality is obtained as

$$\tau_k[n] P_k^{UL}[n] \le \tau_0[n] \Xi(P_0\xi_0). \quad (48)$$

The inequality (48) can be reshaped as follows via an identical deformation

$$-a_k(P_0\xi_0 - b_k) \le \ln\left(\frac{A\tau_0[n]}{(\tau_k[n]P_k^{UL}[n] + \tau_0[n]Y_k)X_k} - 1\right). \quad (49)$$

And finally, the optimization problem P4 can be summarized as follows,

$$\text{P4.1}: \max_{E_0, P_k^{UL}} \sum_{n=1}^{N}\sum_{k=1}^{K} \tau_k[n] \log(1 + \frac{P_k^{UL}[n]\xi}{\sigma^2}), \quad (50a)$$

$$s.t. \quad rank(E_0)=1, \quad (50b)$$

$$||E_0||=1, \quad (50c)$$

$$(43c),(49), \quad (50d)$$

The optimization problem P4.1 is a joint convex problem with linear constraints. This optimization problem can be solved by relaxing the rank one constraint using convex optimization solvers. The relaxation of the rank-one constraint helps obtain an upper bound of the idealized performance and can be used for evaluating the performances of other suboptimal algorithms. Gaussian randomization can be used to obtain a rank one solution if the output optimal solution does not satisfy the constraint of rank one.

To find the solution to problem P0, an iterative algorithm based on AO is proposed. In each iteration, the above four subproblems are sequentially solved in each circulation. The algorithm continues until the predefined precision is satisfied, and thus the final solution is obtained. A summary of the overall optimization algorithm is described by the pseudo code in Algorithm 1.

Algorithm 1 Alternating Optimization Algorithm for Dynamic Phase Shift

1. **Initialization** $L^{(0)}, e_0^{(0)}, e_k{}^{(0)}, \tau_0^{(0)}, \tau_k{}^{(0)}, P_k^{UL(0)}$, let $r = 0, \iota = 10^{-3}$
2. **Repeat**
3. Solve sub-problem 1: given $e_0^{(r)}, e_k{}^{(r)}, \tau_0^{(r)}, \tau_k{}^{(r)}, P_k^{UL(r)}$, obtain $L^{(r+1)}$
4. Solve sub-problem 2: given $L^{(r)}, e_0^{(r)}, \tau_0^{(r)}, \tau_k{}^{(r)}, P_k^{UL(r)}$, obtain $e_k{}^{(r+1)}$
5. Solve sub-problem 3: given $L^{(r)}, e_k{}^{(r)}, e_0^{(r)}, P_k^{UL(r)}$, obtain $\tau_0^{(r+1)}, \tau_k{}^{(r+1)}$
6. Solve sub-problem 4: given $L^{(r)}, e_k{}^{(r)}, \tau_0^{(r)}, \tau_k{}^{(r)}$, obtain $e_0^{(r+1)}, P_k^{UL(r+1)}$
7. Update: $r = r + 1$
8. **Until** Objective function value of (r+1)-th iteration objective function value of r-th iteration $\le \iota$
9. **Return** Optimal values of UAV trajectory, downlink/uplink phase shift, energy/information transmission time, information transmission power

F. COMPLEXITY ANALYSIS

During each iteration, the complexity of problem P1.2 is $O(N)$. The complexity of problems P2 and P3 is $O(M^{3.5})$ [10] and $O(K)$ respectively. The problem P4.1 solves the relaxed SDP problem by the interior point method, so the computational complexity is $O((M+1)^{3.5})$. Assuming that the number of iterations required for the algorithm computational is r, the computational complexity of the proposed algorithm can hence be concluded as $O(r(N + K + M^{3.5} + (M+1)^{3.5}))$.

IV. OPTIMIZATION AND SOLUTION IN THE STATIC PHASE SHIFT SCENARIO

In the static phase shift scenario as shown in Fig.3, the uplink and downlink phase shifts are of the same configurations, so the static phase shift can be set as $\tilde{\Theta}[n] = diag(e^{j\tilde{\theta}_1[n]}, \ldots, e^{j\tilde{\theta}_m[n]})$. Let $e^{j\tilde{\theta}_m[n]} = \tilde{e}_m[n]$. Substitute $\tilde{\Theta}[n]$ to Eq.(21), the following Eq.(51) can be obtained,

$$\tilde{\xi} = \frac{\beta_0 - v_1}{||L[n] - w_k||^\alpha} + \frac{M\beta_0(\beta_0 - v_2)}{||L[n] - w_i||^2 ||w_i - w_k||^\gamma} + |h^I_{U,k}[n] + h^I_{I,k}\tilde{\Theta}[n]h^H_{U,I}[n]|^2. \quad (51)$$

Therefore, the original optimization problem P0 evolves to problem P5.

$$\text{P5}: \max_{\tilde{e}_m, \tau_0, \tau_k, P_k^{UL}, L} R'_{sum} = \sum_{n=1}^{N}\sum_{k=1}^{K} \tau_k[n] \log_2(1 + \frac{P_k^{UL}[n]\tilde{\xi}}{\sigma^2}), \quad (52a)$$

$$s.t. \ (19b)\text{-}(19e),(19f),(19i), \quad (52b)$$

$$|\tilde{e}_m[n]| = 1, m = 1, \ldots, M. \quad (52c)$$

P5 can also be solved by the AO algorithm. Taking into account the main difference of the problem structure between the static and dynamic phase shift problems, the static phase shift optimization algorithm is analyzed in detail. In addition, due to the change of phase shift, Eq. (11) is also changed into $\bar{P}_k^{DL}[n] = P_0|h_{U,k}[n] + h_{I,k}\tilde{\Theta}[n]h_{U,I}[n]|^2$, and substitute it into (30b) to get the new constraint

$$\bar{P}_k^{DL}[n] \geq \Xi^{-1}(\frac{\tau_k[n]}{\tau_0[n]}P_k^{UL}[n]). \tag{53}$$

Given UAV flight trajectory L, energy transfer time τ_0, and information transmission time τ_k, problem P5.1 is hence obtained,

$$\text{P5.1}: \max_{\tilde{e}_m, P_k^{UL}} R'_{sum} \tag{54a}$$

$$s.t.\ (43c),(52c),(53). \tag{54b}$$

The non-concave objective function and non-convex constraint set make problem P5.1 actually a non-convex optimization problem, and auxiliary variables need to be introduced to reshape it. Let $\tilde{e} = [\tilde{e}_1[n], \ldots, \tilde{e}_m[n]]^H$, thus $|h_{U,k}^I[n]+h_{I,k}^I\tilde{\Theta}[n]h_{U,I}^H[n]|^2$ can be written as $|h_{U,k}^I[n] + \tilde{e}^H f_k|^2$. Then we introduce auxiliary variables as

$$\bar{\tilde{e}}_k = \begin{bmatrix} \tilde{e}_k \\ 1 \end{bmatrix}. \tag{55}$$

Therefore, $|h_{U,k}^I[n] + \tilde{e}^H f_k|^2$ can be further expressed as $\bar{\tilde{e}}^H V_k \bar{\tilde{e}} + |h_{U,k}^I[n]|^2$. Since $\bar{\tilde{e}}^H V_k \bar{\tilde{e}} = tr(V_k \bar{\tilde{e}}\bar{\tilde{e}}^H)$, then let $\tilde{E} = \bar{\tilde{e}}\bar{\tilde{e}}^H$, where $\tilde{E} \succcurlyeq 0$ and the rank one constraint must be satisfied, i.e., $Rank(\tilde{E}) = 1$. Thus $\tilde{\xi} = \omega_k + |h_{U,k}^I[n]|^2 + tr(V_k\tilde{E})$. After the above processing, the objective function (52a) becomes a tractable convex function. Lemma 3 is proposed to transform the non-convex rank-one constraint to the deviation of a spectral norm from a kernel norm through the difference-convex (DC) programming.

Lemma 3: For a semi-positive definite square matrix $\mathbf{M}$, the rank-one constraint can be equivalently transformed to the difference of two convex functions, i.e.,

$$Rank(\mathbf{M})=1 \Leftrightarrow ||\mathbf{M}||_* - ||\mathbf{M}||_2 \leq 0, \tag{56}$$

where $||\mathbf{M}||_*$ denotes the kernel norm of the matrix $\mathbf{M}$, which is the sum of the singular values, i.e. $||\mathbf{M}||_* = \sum_{n=1}^{N} \sigma_n(\mathbf{M})$, $\sigma_n(\mathbf{M})$ represents the first n largest singular values, and $||\mathbf{M}||_2$ denotes the spectral norm of the matrix, i.e. $||\mathbf{M}||_2 = \sigma_1(\mathbf{M})$.

Proof: For any m-dimensional Hermitian matrix, $||\mathbf{M}||_* \geq ||\mathbf{M}||_2$ is established. The equality holds if and only if the rank of $\mathbf{M}$ is 1. The proof of **Lemma 3** is completed.

Consequently, the kernel and spectral norm can be used to equivalently represent the rank one constraint. Thus, the equivalently transformed rank one constraint is added to the objective function as a penalty term [37] according to Lemma 3, the problem P5.1 now evolves to P5.2.

$$\text{P5.2}: \max_{\tilde{E}, P_k^{UL}} R'_{sum} + \frac{1}{\mu}(||\tilde{E}||_* - ||\tilde{E}||_2), \tag{57a}$$

$$s.t.\ P_0(\omega_k + |h_{U,k}^I[n]|^2 + tr(V_k\tilde{E})) \geq \Xi^{-1}(\frac{\tau_k[n]}{\tau_0[n]}P_k^{UL}[n]), \tag{57b}$$

$$\tilde{E} \succcurlyeq 0, \tag{57c}$$

$$(52c). \tag{57d}$$

In this case, μ is the penalty factor, and the objective function is expressed in the form of DC, which can be solved by using SCA. The lower bound of $||\tilde{E}||_2$ in the objective function of P5.2 can be estimated by the first-order Taylor expansion at each iteration of the SCA algorithm which is shown as

$$||\tilde{E}||_2 \geq ||\tilde{E}^{(r)}||_2 + tr[\lambda_{\max}(\tilde{E}^{(r)}) \times \lambda_{\max}^H(\tilde{E}^{(r)})(\tilde{E} - \tilde{E}^{(r)})], \tag{58}$$

where $\tilde{E}^{(r)}$ is the solution obtained at the r-th iteration. Updating the objective function with its lower bound, the optimization problem P5.2 can be rewritten as P5.3,

$$\text{P5.3}: \max_{\tilde{E}, P_k^{UL}} R'_{sum} + \frac{1}{\mu}(||\tilde{E}||_* - ||\tilde{E}^{(r)}||_2 - tr[\lambda_{\max}(\tilde{E}^{(r)}) \times \lambda_{\max}^H(\tilde{E}^{(r)})(\tilde{E} - \tilde{E}^{(r)})], \tag{59a}$$

$$s.t.\ (57b)\text{-}(57d). \tag{59b}$$

Algorithm 2 Optimization Algorithm Design for Static Phase Shift

1. **Initialization** $L^{(0)}, \tilde{e}_m^{(0)}, \tau_0^{(0)}, \tau_k{}^{(0)}, P_k^{UL(0)}$, let $r = 0, \iota = 10^{-3}$
2. **Repeat**
3. Solve sub-problem 1: given $e_0^{(r)} = e_k{}^{(r)} = \tilde{e}_m^{(r)}, \tau_0^{(r)}, \tau_k{}^{(r)}, P_k^{UL(r)}$, obtain $L^{(r+1)}$
4. Solve sub-problem 3: given $L^{(r)}, e_0^{(r)} = e_k{}^{(r)} = \tilde{e}_m^{(r)}, P_k^{UL(r)}$, obtain $\tau_0^{(r+1)}, \tau_k{}^{(r+1)}$
5. Solve sub-problem 5: given $L^{(r)}, \tau_0^{(r)}, \tau_k{}^{(r)}$, obtain $\tilde{e}_m^{(r+1)}, P_k^{UL(r+1)}$
6. Update: $r = r + 1$
7. **Until** Objective function value of (r+1)-th iterationobjective function value of r-th iteration $\leq \iota$
8. **Return** Optimal values of UAV trajectory, static phase shift, energy/information transmission time, information transmission power

This problem can be directly solved by using the CVX toolbox, because it is now a convex optimization problem with respect to $\tilde{E}$ and P_k^{UL}. Algorithm 2 summarizes the process for getting the optimal solution in scenario of static phase shift.

V. SIMULATION RESULTS AND PERFORMANCE EVALUATIONS

This section provides numerical results to verify the effectiveness of the two proposed algorithms and analyzes their performance gap in WPCN with the aid of UAV and IRS. Consider a UAV hovering at a fixed height of 80m, a maximum flight speed of 20m/s, and a transmitting power of 40dBm. The UAV's initial and termination projection coordinates are (0, 0) and (500m, 0) respectively. The IRS is mounted at a height of 30m with its projection coordinate (250m, 250m), and the number of reflection elements of the IRS is set to be 50. Signal attenuation is set as 30dB when the reference distance $\beta_0 = 1$m. The other parameters for all K wireless devices are assigned with uniformly the same values, i.e., $A = 24$mV, $a_k = 150$, $b_k = 0.024$ [38], Rician factor κ_1=κ_2=3dB. The AWGN is $\sigma = -80$dBm, and the algorithm's precision value ι is 10^{-3}.

Fig.4 shows four flight trajectories of UAV along their tracks with different time constraints in the dynamic phase shift scenario. By observing Fig.4, the trajectory of UAV varies with time constraints. When the hovering time T gets longer, UAV approaches closer to the geometric center of wireless devices' locations to help reduce the link length between them, by which better DL-WPT and UL-WIT channel gains can be obtained. Due to the merits of IRS, UAV prefers to move towards it to readjust the existed relay links and the directed links. When the hovering time is set as $T = 80$s, UAV will spend more time on circling over the IRS to provide better service quality to wireless devices planted on the ground. However, in the none-IRS case without time limits, UAV flight trajectory obviously changes. UAV will approach to the point just over the uppermost device to promote better channel conditions.

Figure 5 shows the time separation for WPT and WIT when $T = 60$s and $T = 80$s, respectively. It is interesting to find that HAP is more likely to serve less devices rather than serving all devices once upon a segment. When HAP maintains to serve one device, the time used for WPT will decrease as T increases. In another word, when the energy reserve of the device is insufficient, HAP will spend more time on energy transferring, whereas when the energy reserve is sufficient, HAP will allocate more time on WIT. In the extreme cases, the time length for energy transmission can be optimally reduced to 0 in specific time segment.

Fig.6 shows the relationship between the number of IRS reflective elements and the achievable sum rate when $P_0 = 50$dBm, $k = 6$. The proposed two schemes, dynamic phase shift and static phase shift, achieve visibly higher network throughput than those of the random IRS phase shift scheme and the none-IRS scheme when varying the number of M from 20 to 100. Compared with the IRS-WPCN algorithm proposed in [10], the dynamic phase shift scheme increased in the network throughput by about 28 percent with the same simulation settings. Moreover, the network throughput brought by the dynamic phase shift is increased up by about five times to the proposal for UAV-WPCN in [18].

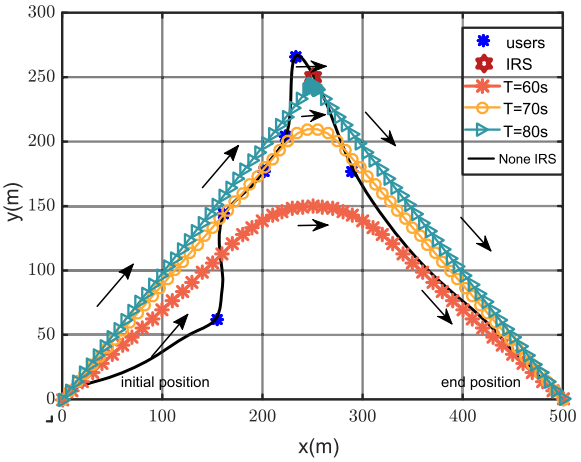

FIGURE 4. UAV's trajectory projected on the horizontal plane.

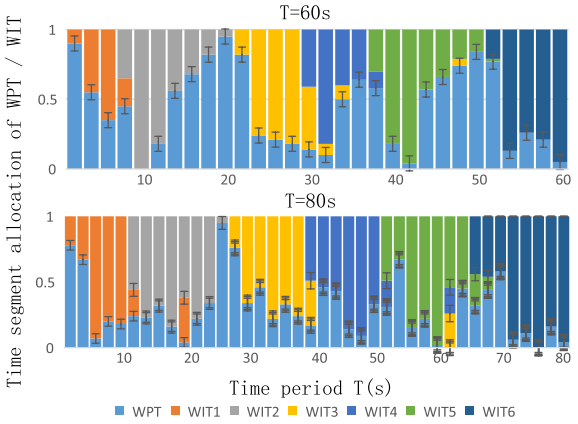

FIGURE 5. Time segment allocation histogram.

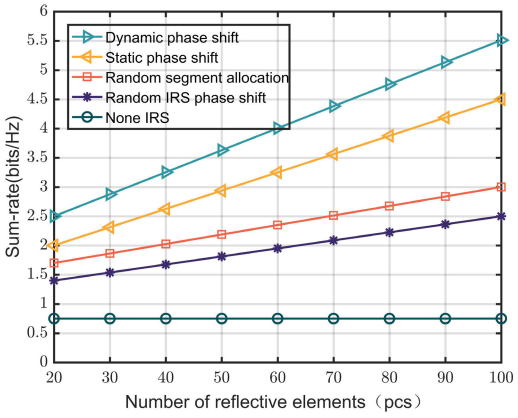

FIGURE 6. The relationship between the sum rate and the number of reflective elements.

As seen from the above facts, single technique, i.e., solely UAV and IRS, is confined in effectively improving the network throughput of WPCN. Moreover, it can be observed that the random segment allocation scheme can achieve higher throughput than that of the random IRS phase shift scheme, because the reflected signal of indirect link will experience poor channel gain in the random phase shift, and ultimately reduce the total network throughput. In contrast, the random segment allocation will affect the time of energy collection

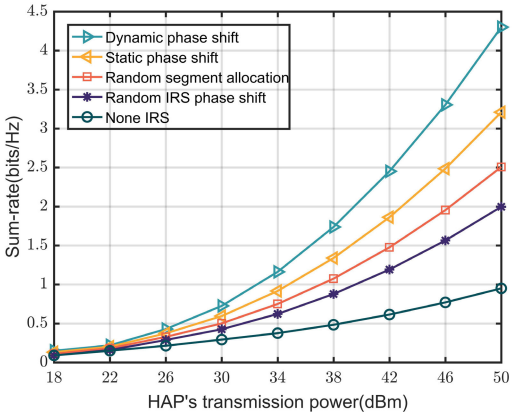

FIGURE 7. The relationship between the sum rate and the HAP transmission power.

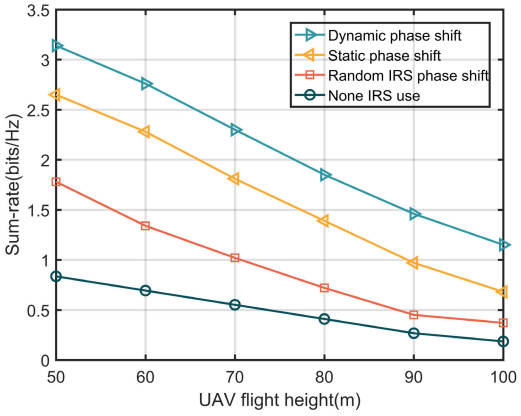

FIGURE 8. The relationship between the sum rate and the UAV's flight height.

and information transmission. That is to say, the device needs more transmitting power, or the information transmission time has to be longer, leading to a trivial increase of the network throughput. The sum rate of the proposed two IRS phase-shift optimization schemes, increases monotonically with M, since more reflective elements promote greater growth. In addition, the sum rate performance gap between the proposed two schemes becomes evident as M increases. That is because the static phase shift scheme in DL or UL prevents the IRS from releasing its entire beamforming gain. This demonstrates the necessity for dynamic phase shifting in the applications of large-scale deployment of IRS.

Fig.7 shows the effect of the UAV transmission power P_0 on the sum rate when $M = 50$. It can be seen from Fig.7 that the sum rate rises with the increase of P_0 in all the selected schemes. Nevertheless, increasing transmission power results in the rise of the sum rate but at the cost of excessive energy consumption at the UAV (HAP). When considering the UAV's limited energy reserves, increasing transmission power is not economical to raise the rate for a green and sustainable WPCN. It is also found that the IRS with random phase shift obtains a lower sum rate increase than that of the none-IRS assistance scheme, because the reflective links assisted by the IRS have been compensated by the worse channel gain resulting from the randomly signals bounced back by the IRS.

The relationship between the UAV's flight height and the sum rate is shown in Fig.8 when $M = 50$, $P_0 = 50$dBm. It describes that when the height of the UAV rises, the sum rate descends. Correspondingly, when the UAV's fight height descends from 100m to 50m, the UAV gets much closer to the devices on the ground. Thus the air-ground channel quality is improved, and the energy transfer efficiency improves, leading to the sum rate rising rapidly.

VI. CONCLUSION

The paper aims at maximizing the the network throughput of UAV-WPCN with the aid of IRS. The UAV flight trajectory, uplink and downlink phase shifts of IRS, transmission time, and transmission power of the UAV are jointly optimized. The IRS's dynamic and static phase shifts are studied separately to analyze their network performance gap. To solve the formulated non-convex optimization problems, successive convex approximation, difference-convex optimization, and penalty functions are applied. Numerical simulation results validate the effectiveness and convergence of the proposed algorithms. The results disclose that the conjunctive use of UAV and IRS can effectively improve the network throughput of UAV-WPCN at a low cost.

APPENDIX A PROOF OF LEMMA 1

Let $f(x) = \log_2(1+x), x > 0, g(x) = \log_2(1+\frac{1}{x}), x > 0$. Clearly, $f(x)$ is a concave function for x and $g(x)$ is a convex function for x. We get the following inequality based on Jensen's inequality [39],

$$\log_2(1+\frac{1}{E\{1/x\}}) \le E\{\log_2(1+x)\} \le \log_2(1+E\{x\}). \tag{1}$$

Let $x = A/B, A > 0, B > 0$, then obtain

$$\log_2(1+\frac{1}{E\{B/A\}}) \le E\{\log_2(1+A/B)\} \le \log_2(1+E\{A/B\}). \tag{2}$$

If $A > 0, B > 0$ are independent of each other, then

$$E\{A/B\} = E\{A\}E\{1/B\} \ge E\{A\}/E\{B\}. \tag{3}$$

where the inequality holds due to the convexity of function $1/B$ for $B > 0$ and Jensen's inequality. As a result, equation (3) gives us

$$\begin{aligned}\log_2(1+\frac{1}{E\{B/A\}}) &\le \log_2(1+E\{A\}/E\{B\}) \\ &\le \log_2\{1+E\{A/B\}\}.\end{aligned} \tag{4}$$

The comparison of equations (2) and (4) show that $E\{\log_2(1+A/B)\}$ and $\log_2(1+E\{A\}/E\{B\})$ have the same upper and lower bounds. We can obtain $E\{\log_2(1+A/B)\} = \log_2(1+E\{A\}/E\{B\}) = 0$ when $A = 0, B > 0$ occurs. Consequently, there are similar results expressed by equation (20).

REFERENCES

[1] K. Shafique, B. A. Khawaja, F. Sabir, S. Qazi, and M. Mustaqim, "Internet of Things (IoT) for next-generation smart systems: A review of current challenges, future trends and prospects for emerging 5G-IoT scenarios," *IEEE Access*, vol. 8, pp. 23022–23040, 2020.

[2] T. Nguyen, V. Nguyen, J. Lee, and Y. Kim, "Sum rate maximization for multi-user wireless powered IoT network with non-linear energy harvester: Time and power allocation," *IEEE Access*, vol. 7, pp. 149698–149710, 2019.

[3] D. Xu and H. Zhu, "Secure transmission for SWIPT IoT systems with full-duplex IoT devices," *IEEE Internet Things J.*, vol. 6, no. 6, pp. 10915–10933, Dec. 2019.

[4] L. R. Varshney, "Transporting information and energy simultaneously," in *Proc. IEEE Int. Symp. Inf. Theory*, Toronto, ON, Canada, Jul. 2008, pp. 1612–1616.

[5] Y. Shen, K. Kwak, B. Yang, and S. Wang, "Subcarrier-pairing-based resource optimization for OFDM wireless powered relay transmissions with time switching scheme," *IEEE Trans. Signal Process.*, vol. 65, no. 5, pp. 1130–1145, Mar. 2017.

[6] Q. Wu, G. Y. Li, W. Chen, D. W. K. Ng, and R. Schober, "An overview of sustainable green 5G networks," *IEEE Wireless Commun.*, vol. 24, no. 4, pp. 72–80, Aug. 2017.

[7] Q. Wu and R. Zhang, "Weighted sum power maximization for intelligent reflecting surface aided SWIPT," *IEEE Wireless Commun. Lett.*, vol. 9, no. 5, pp. 586–590, May 2020.

[8] M. Hua and Q. Wu, "Joint dynamic passive beamforming and resource allocation for IRS-aided full-duplex WPCN," *IEEE Trans. Wireless Commun.*, vol. 21, no. 7, pp. 4829–4843, Jul. 2022.

[9] H. Cao, Z. Li, and W. Chen, "Resource allocation for IRS-assisted wireless powered communication networks," *IEEE Wireless Commun. Lett.*, vol. 10, no. 11, pp. 2450–2454, Nov. 2021.

[10] H. Ju and R. Zhang, "Throughput maximization in wireless powered communication networks," *IEEE Trans. Wireless Commun.*, vol. 13, no. 1, pp. 418–428, Jan. 2014.

[11] Q. Wu, X. Zhou, W. Chen, J. Li, and X. Zhang, "IRS-aided WPCNs: A new optimization framework for dynamic IRS beamforming," *IEEE Trans. Wireless Commun.*, vol. 21, no. 7, pp. 4725–4739, Jul. 2022.

[12] S. Zhang, Q. Wu, S. Xu, and G. Y. Li, "Fundamental green tradeoffs: Progresses, challenges, and impacts on 5G networks," *IEEE Commun. Surveys Tuts.*, vol. 19, no. 1, pp. 33–56, 1st Quat., 2017.

[13] T. Cui, M. Qi, and X. Wan, "Coding metamaterials, digital metamaterials and programmable metamaterials," *Light, Sci. Appl.*, vol. 3, no. 10, p. e281, Oct. 2014.

[14] Q. Wu and R. Zhang, "Towards smart and reconfigurable environment: Intelligent reflecting surface aided wireless network," *IEEE Commun. Mag.*, vol. 58, no. 1, pp. 106–112, Jan. 2020.

[15] W. Tang, "Wireless communications with reconfigurable intelligent surface: Path loss modeling and experimental measurement," *IEEE Trans. Wireless Commun.*, vol. 20, no. 1, pp. 421–439, Jan. 2021.

[16] P. S. Bithas, V. Nikolaidis, A. G. Kanatas, and G. K. Karagiannidis, "UAV-to-ground communications: Channel modeling and UAV selection," *IEEE Trans. Commun.*, vol. 68, no. 8, pp. 5135–5144, Aug. 2020.

[17] Q. Wu, Y. Zeng, and R. Zhang, "Joint trajectory and communication design for multi-UAV enabled wireless networks," *IEEE Trans. Wireless Commun.*, vol. 17, no. 3, pp. 2109–2121, Mar. 2018.

[18] W. Wang, "Joint precoding optimization for secure SWIPT in UAV-aided NOMA networks," *IEEE Trans. Commun.*, vol. 68, no. 8, pp. 5028–5040, Aug. 2020.

[19] J. Park, H. Lee, S. Eom, and I. Lee, "UAV-aided wireless powered communication networks: Trajectory optimization and resource allocation for minimum throughput maximization," *IEEE Access*, vol. 7, pp. 134978–134991, 2019.

[20] L. Xie, J. Xu, and R. Zhang, "Throughput maximization for UAV-enabled wireless powered communication networks," *IEEE Internet Things J.*, vol. 6, no. 2, pp. 1690–1703, Apr. 2019.

[21] J. Xu, Y. Zeng, and R. Zhang, "UAV-enabled wireless power transfer: Trajectory design and energy optimization," *IEEE Trans. Wireless Commun.*, vol. 17, no. 8, pp. 5092–5106, Aug. 2018.

[22] Z. Chen, K. Chi, K. Zheng, G. Dai, and Q. Shao, "Minimization of transmission completion time in UAV-enabled wireless powered communication networks," *IEEE Internet Things J.*, vol. 7, no. 2, pp. 1245–1259, Feb. 2020.

[23] B. Lyu, P. Ramezani, D. T. Hoang, S. Gong, Z. Yang, and A. Jamalipour, "Optimized energy and information relaying in self-sustainable IRS-empowered WPCN," *IEEE Trans. Commun.*, vol. 69, no. 1, pp. 619–633, Jan. 2021.

[24] Z. Li, W. Chen, Q. Wu, H. Cao, K. Wang, and J. Li, "Robust beamforming design and time allocation for IRS-assisted wireless powered communication networks," *IEEE Trans. Commun.*, vol. 70, no. 4, pp. 2838–2852, Apr. 2022.

[25] T. Li, P. Fan, Z. Chen, and K. B. Letaief, "Optimum transmission policies for energy harvesting sensor networks powered by a mobile control center," *IEEE Trans. Wireless Commun.*, vol. 15, no. 19, pp. 6132–6145, Sep. 2016.

[26] J. Tang, J. Song, J. Ou, J. Luo, X. Zhang, and K.-K. Wong, "Minimum throughput maximization for multi-UAV enabled WPCN: A deep reinforcement learning method," *IEEE Access*, vol. 8, pp. 9124–9132, 2020.

[27] Z. Li, W. Chen, H. Cao, H. Tang, K. Wang, and J. Li, "Joint communication and trajectory design for intelligent reflecting surface empowered UAV SWIPT networks," *IEEE Trans. Veh. Technol.*, vol. 71, no. 12, pp. 12840–12855, Dec. 2022.

[28] B. Zheng and R. Zhang, "Intelligent reflecting surface-enhanced OFDM: Channel estimation and reflection optimization," *IEEE Wireless Commun. Lett.*, vol. 9, no. 4, pp. 518–522, Apr. 2020.

[29] N. Senadhira, S. Durrani, X. Zhou, N. Yang, and M. Ding, "Uplink NOMA for cellular-connected UAV: Impact of UAV trajectories and altitude," *IEEE Trans. Commun.*, vol. 68, no. 8, pp. 5242–5258, Aug. 2020.

[30] X. Chen, J. Shi, Z. Yang, and L. Wu, "Low-complexity channel estimation for intelligent reflecting surface-enhanced massive MIMO," *IEEE Wireless Commun. Lett.*, vol. 10, no. 5, pp. 996–1000, May 2021.

[31] S. Liu, Z. Gao, J. Zhang, M. D. Renzo, and M.-S. Alouini, "Deep denoising neural network assisted compressive channel estimation for mmWave intelligent reflecting surfaces," *IEEE Trans. Veh. Technol.*, vol. 69, no. 8, pp. 9223–9228, Aug. 2020.

[32] K. Xiong, B. Wang, and K. J. R. Liu, "Rate-energy region of SWIPT for MIMO broadcasting under nonlinear energy harvesting model," *IEEE Trans. Wireless Commun.*, vol. 16, no. 8, pp. 5147–5161, Aug. 2017.

[33] J. Bezdek and R. Hathaway, "Some notes on alternating optimization," in *Proc. AFSS Int. Conf. Fuzzy Syst.*, Feb. 2002, pp. 187–195.

[34] C. James and J. Richard, "Convergence of alternating optimization," *Neural, Parallel Sci. Computations*, vol. 11, no. 4, Dec. 2003, Art. no. 351368.

[35] M. Grant, S. Boyd, (2014). *CVX: MATLAB Software for Disciplined Convex Programming, Version 2.1*. [Online]. Available: http://cvxr.com/cvx/

[36] S. Sun, M. Fu, Y. Shi, and Y. Zhou, "Towards reconfigurable intelligent surfaces powered green wireless networks," in *Proc. IEEE Wireless Commun. Netw. Conf. (WCNC)*, May 2020, pp. 1–6.

[37] X. Yu, D. Xu, Y. Sun, D. W. K. Ng, and R. Schober, "Robust and secure wireless communications via intelligent reflecting surfaces," *IEEE J. Sel. Areas Commun.*, vol. 38, no. 11, pp. 2637–2652, Nov. 2020.

[38] Y. Lu, K. Xiong, P. Fan, Z. Ding, Z. Zhong, and K. Letaief, "Global energy efficiency in secure MISO SWIPT systems with non-linear power-splitting EH model," *IEEE J. Sel. Areas Commun.*, vol. 37, no. 1, pp. 216–232, Jan. 2019.

[39] J. Lu, Y. Wang, Y. Chen, and H. Jia, "Joint UAV deployment and energy transmission design for throughput maximization in IoRT networks," in *Proc. IEEE/CIC Int. Conf. Commun. China (ICCC)*, Jul. 2021, pp. 236–241.

LIANG XUE (Member, IEEE) received the B.S., M.S., and Ph.D. degrees in control theory and engineering from Yanshan University, Qinhuangdao, China, in 2006, 2009, and 2012, respectively. He is currently a Professor with the School of Information and Electrical Engineering and the Chair of the Department of Internet of Things, Hebei University of Engineering, Handan, China. He is also the Outstanding Young Scholar of Hebei Education Department and Hebei new century "333 Talent Project" third-level suitable person. From June 2017 to June 2018, he was a Visiting Scholar with the Cyber Network Security Group, Arizona State University, USA. He is currently in charge of several research projects, including the National Natural Science Foundation of China, the Natural Science Foundation of Hebei Province, and the Scientific Research Plan of Hebei Education Department. His research interests include the clustering design, hierarchical topology control, data routing in wireless sensor networks, and wireless cognitive radio networks.

XUAN GONG (Student Member, IEEE) received the B.S. degree in computer science and technology from Taishan University, Tai'an, China, in 2020. He is currently pursuing the M.S. degree in computer science and technology with the Hebei University of Engineering, Handan, China. His research interests include wireless powered communication networks, intelligent reflecting surface, and simultaneous wireless information and power transfer.

YANYAN SHEN (Member, IEEE) received the B.S. and M.Eng. degrees in electrical engineering from Yanshan University, Qinhuangdao, China, in 2006 and 2009, respectively, and the Ph.D. degree from the Department of Mechanical and Biomedical Engineering, City University of Hong Kong, Hong Kong, SAR, China, in 2012. From 2013 to 2014, she was a Postdoctoral Research Fellow with the School of Information and Communication Engineering, Inha University, South Korea. She is currently an Associate Professor with the Shenzhen Institute of Advanced Technology, Chinese Academy of Sciences, Shenzhen, China. She has been the principal investigator/the co-investigator in several research projects funded by NSFC and Shenzhen Basic Research Foundation. Her current research interests include wireless energy harvesting, UAV communications, mobile edge computing, and intelligent resource management in next generation networks.

BALAJI PANCHAL received the Ph.D. degree in biochemistry from Dr. Babasaheb Ambedkar Marathwada University, Aurangabad, Maharashtra, India, in 2016. He was a Postdoctoral Scientist with the Key Laboratory of Resource Exploration Research of Hebei Province, Hebei University of Engineering, Handan, Hebei, China. His current research interests include biomedical signal measurement, biomedical signal processing, and ecological resources and materials.

CHUN-JIE WANG received the B.S. degree in computer science and technology from the Henan Institute of Engineering, Zhengzhou, China, in 2021. He is currently pursuing the M.S. degree in computer science and technology with the Hebei University of Engineering, Handan, China. From June 2022 to June 2024, he was a Visiting Scholar with the Institute of Advanced Computing and Digital Engineering, Shenzhen Institute of Advanced Technology, Chinese Academy of Science. His research interests include intelligent reflecting surface, simultaneous wireless information and power transfer, and unmanned aerial vehicle communication.

YAN-LONG WANG received the B.S. degree in computer science and technology from the Hebei University of Architecture, Zhangjiakou, China, in 2011, and the M.S. degree in information and electric engineering from the Hebei University of Engineering, Handan, China, in 2015. He is currently pursuing the Ph.D. degree with the Key Laboratory of Trustworthy Distributed Computing and Service, Beijing University of Posts and Telecommunications, Beijing, China. His research interests include simultaneous wireless information, power transfer, and network security.